

Zero-bias states and the mechanism of the surface $d \rightarrow d+is$ transition

Simon Kos

University of Illinois, Department of Physics, 1110 West Green Street, Urbana, Illinois 61801

(Received 22 September 2000; revised manuscript received 13 December 2000; published 7 May 2001)

We study the physical mechanism of the surface $d \rightarrow d+is$ transition. We base our argument on first-order perturbation theory and show that the zero-bias states drive the transition. We support the argument by various estimates and consistency checks.

DOI: 10.1103/PhysRevB.63.214506

PACS number(s): 74.50.+r, 74.25.Bt, 74.20.-z

I. INTRODUCTION

Many researchers presently believe that the order parameter in the hole-doped cuprate superconductors has a predominant d -wave symmetry.¹ Due to this symmetry, an inhomogeneity may scatter a quasiparticle between directions with opposite signs of the superconducting order parameter Δ . The Atiyah-Patodi-Singer index theorem² then implies that for each such trajectory, the Andreev Hamiltonian has a normalizable eigenstate of zero energy, so called zero-bias state (ZBS) irrespective of the detailed shape of Δ . This effect is strongest for the specularly reflecting (110) surface. As Fig. 1 shows, Δ in this case changes sign upon reflection along every quasiclassical trajectory. This gives rise to a zero-bias peak in the local density of states as was realized by Hu.³

Matsumoto and Shiba⁴ were the first to suggest that the spontaneous appearance of the order parameter component of different symmetry, say s or d_{xy} close to the surface phase-shifted by $\pi/2$ relative to the dominant $d_{x^2-y^2}$ might move the ZBS's away from $E=0$. The resultant “ $d+is$ ” or “ $d+id$ ” state breaks time-reversal symmetry. Fögelstrom *et al.*⁵ then included surface roughness and worked out the phase diagram. The calculations^{4,5} were carried out in the Eilenberger formalism.⁶ The Eilenberger function is essentially the local Green's function in the quasiclassical approximation, so it contains contributions from all the states in the spectrum. Hence, the Eilenberger formalism does not show which states drive the transition, especially if the equations are solved numerically. Hence, we use the Andreev formalism⁷ that *does* study the eigenstates individually. We show that the transition is driven by the ZBSs *only*. This is the main result of the present paper.

A number of tunneling experiments⁸⁻¹¹ have observed the zero-bias peak predicted by Hu. In optimally doped $\text{YBa}_2\text{Cu}_3\text{O}_{7-\delta}$ (YBCO), the peak splits at low temperatures,¹² but experiments with Josephson junctions and SQUIDs failed to detect the magnetic field spontaneously created in the state with broken time-reversal symmetry.¹⁴ If we want to compare theory to experiments, we have to remember that s and $d_{x^2-y^2}$ mix freely in YBCO due to orthorhombicity, but d_{xy} and $g_{xy(x^2-y^2)}$ are incompatible with them, as follows from group-theoretical arguments^{15,16} and has been observed by tunneling.^{17,18} Hence, the actual transition would be more accurately described as $\Delta_1 \rightarrow \Delta_1 + i\Delta_2$, where Δ_1 is a real, linear combination of s and $d_{x^2-y^2}$ -wave order-parameter components,

and Δ_2 is a real, linear combination of d_{xy} and $g_{xy(x^2-y^2)}$ -wave order-parameter components. Further, we should take into account the possibility of formation of magnetic domains indicated by recent ESR measurements.¹⁹ We should also consider corrections to the quasiclassical approximation which are of the order $\Delta^2/E_F \sim 3$ meV, and, perhaps, even corrections to the mean-field BCS approximation since the cuprates are strongly-correlated systems. All these complications would make our calculation and results more realistic, but would obscure the main point, i.e., the role of the ZBSs in the transition. Hence, we will illustrate the basic physical mechanism of the transition on the simplified model used previously^{4,5} of a half CuO_2 plane with the dominant and subdominant pairing having pure $d_{x^2-y^2}$ and s symmetry respectively (as if the cuprate were tetragonal, in which case the $d_{x^2-y^2}$ and s symmetries do not mix^{15,16}), and with translational invariance parallel to the boundary. To give a feeling for how much physics is captured by this simplest model, we provide order-of-magnitude estimates for various quantities.

The paper is organized as follows. In Sec. II, we demonstrate our strategy on the familiar case of BCS instability. The main argument is presented in Sec. III after we have extended the BCS formalism to inhomogeneous systems and non- s -wave pairing. Based on this argument, we calculate Δ at $T=0$ in Sec. IV and estimate the transition temperature to the $d+is$ state in Sec. V. In Sec. VI, we discuss the surface current. Finally, we discuss our results in Sec. VII.

II. BCS INSTABILITY

There are various ways to consider the energetic costs and benefits of the transition to the superfluid state. The one that

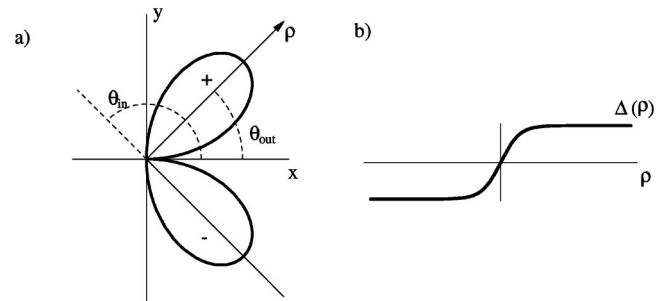


FIG. 1. (a) A schematic picture of the normal metal-superconductor junction in the (110) direction with a typical quasiclassical trajectory. (b) A schematic graph of the pairing potential along the trajectory in (a).

has proven useful in our study of the $d \rightarrow d+is$ transition is to decouple the attractive four-fermion interaction by the Hubbard-Stratonovich (HS) transformation, and to make a saddle-point (mean-field) approximation. That way, we break up the total free energy of the system into free energy of single particle states, which is lowered by the gap Δ , and the extra term from the HS transformation, which grows (quadratically) with Δ . We then see that at small enough T , the system favors transition to the superfluid state.

We will demonstrate this on the familiar BCS case. The model Hamiltonian is (since there is no universal convention as to whether the attractive interaction term should have a plus sign with a negative coupling constant V or a minus sign with positive V , we use $|V|$ which is unambiguously positive)

$$H = \sum_{\mathbf{k}, \sigma} \epsilon_{\mathbf{k}} c_{\mathbf{k}, \sigma}^{\dagger} c_{\mathbf{k}, \sigma} - |V| \sum_{\mathbf{k}, \mathbf{k}'} c_{\mathbf{k}\uparrow}^{\dagger} c_{-\mathbf{k}\downarrow}^{\dagger} c_{-\mathbf{k}'\downarrow} c_{\mathbf{k}'\uparrow}, \quad (2.1)$$

which gives rise to the partition function

$$Z = \int \mathcal{D}\bar{c}_{\mathbf{k}\sigma} \mathcal{D}c_{\mathbf{k}\sigma} \exp - \int_0^{\beta} d\tau \left[\sum_{\mathbf{k}\sigma} \bar{c}_{\mathbf{k}\sigma} (\partial_{\tau} + \epsilon_{\mathbf{k}}) c_{\mathbf{k}\sigma} - |V| \sum_{\mathbf{k}, \mathbf{k}'} \bar{c}_{\mathbf{k}\uparrow} \bar{c}_{-\mathbf{k}\downarrow} c_{-\mathbf{k}'\downarrow} c_{\mathbf{k}'\uparrow} \right], \quad (2.2)$$

where the c 's are now τ -dependent Grassmann numbers. We perform the HS transformation by multiplying the partition function by the (infinite) constant

$$\int \mathcal{D}\bar{\phi}_{\mathbf{k}} \mathcal{D}\phi_{\mathbf{k}} e^{-|V| \int_0^{\beta} d\tau \sum_{\mathbf{k}, \mathbf{k}'} (\bar{\phi}_{\mathbf{k}} - \bar{c}_{\mathbf{k}\uparrow} \bar{c}_{-\mathbf{k}\downarrow}) (\phi_{\mathbf{k}'} - c_{-\mathbf{k}'\downarrow} c_{\mathbf{k}'\uparrow})},$$

so

$$Z = \int \mathcal{D}\bar{\phi}_{\mathbf{k}} \mathcal{D}\phi_{\mathbf{k}} \mathcal{D}\bar{c}_{\mathbf{k}\sigma} \mathcal{D}c_{\mathbf{k}\sigma} e^{-S}, \quad (2.3)$$

where

$$S = \int_0^{\beta} d\tau \left[\sum_{\mathbf{k}} \begin{pmatrix} \bar{c}_{\mathbf{k}\uparrow} & c_{-\mathbf{k}\downarrow} \end{pmatrix} \begin{pmatrix} \partial_{\tau} + \epsilon_{\mathbf{k}} & \Delta \\ \bar{\Delta} & \partial_{\tau} - \epsilon_{\mathbf{k}} \end{pmatrix} \begin{pmatrix} c_{\mathbf{k}\uparrow} \\ \bar{c}_{-\mathbf{k}\downarrow} \end{pmatrix} + \frac{|\Delta|^2}{|V|} \right], \quad (2.4)$$

where we defined

$$\Delta = -|V| \sum_{\mathbf{k}} \phi_{\mathbf{k}}.$$

From the action (2.4), we can read off that in the mean-field approximation, the total free energy of the system is given by the Ginzburg-Landau functional

$$F(|\Delta|) = \sum_{\mathbf{k}} [\mathcal{F}(E_{\mathbf{k}}) + \mathcal{F}(-E_{\mathbf{k}})] + \frac{|\Delta|^2}{|V|} \quad (2.5)$$

upon minimization with respect to $|\Delta|$. Here,

$$\mathcal{F}(E) = -T \ln(1 + e^{-E/T}) \quad (2.6)$$

and

$$E_{\mathbf{k}} = \sqrt{\epsilon_{\mathbf{k}}^2 + |\Delta|^2}.$$

We see the instability most clearly at $T=0$, where $F(|\Delta|) = E(|\Delta|)$. Then

$$\mathcal{F}(E) = \theta(-E)E,$$

so

$$E(|\Delta|) - E(0) = 2N(0) \int_{-\omega_D}^0 d\epsilon (-\sqrt{\epsilon^2 + |\Delta|^2} - \epsilon) + \frac{|\Delta|^2}{|V|}, \quad (2.7)$$

where $N(0)$ is the density of states at the Fermi level and ω_D is the Debye frequency. Direct calculation shows that the integral behaves as $|\Delta|^2 \ln(|\Delta|/\omega_D)$ for $|\Delta| \rightarrow 0$, whose nonanalytic decrease will win over the analytic increase of the second term for small enough Δ , no matter how weak the attractive interaction $|V|$ is. By the same calculation, we can also see that the integral becomes analytic if we do not integrate ϵ all the way up to zero, but to a finite negative energy. This means that the states close to the Fermi energy drive the BCS transition—they benefit most from opening of the gap $|\Delta|$. Similarly, we shall see that the states at zero energy, that is the ZBS's, will drive the $d \rightarrow d+is$ transition.

So far, the argument has shown the BCS instability only at $T=0$. At finite temperatures,

$$\mathcal{F}(E_{\mathbf{k}}) + \mathcal{F}(-E_{\mathbf{k}}) = -T \ln \left(2 + 2 \cosh \frac{E_{\mathbf{k}}}{T} \right),$$

which gives the Ginzburg-Landau expansion in powers of $|\Delta|^2$

$$F(|\Delta|) - F(0) = |\Delta|^2 \left(\frac{1}{|V|} - N(0) \int_{-\omega_D}^0 \frac{d\epsilon}{\epsilon} \tanh \frac{\epsilon}{2T} \right) + |\Delta|^4 \left(\frac{-N(0)}{4} \right) \int_{-\omega_D}^0 \frac{d\epsilon}{\epsilon} \frac{d}{d\epsilon} \left(\frac{1}{\epsilon} \tanh \frac{\epsilon}{2T} \right) + O(|\Delta|^6). \quad (2.8)$$

The function $(1/\epsilon) \tanh(\epsilon/2T)$ is positive and monotonically increasing for $\epsilon < 0$, so the integral in the quadratic coefficient is positive and the integral in the quartic coefficient is negative for any $T > 0$. Hence, close to the temperature T_c that satisfies

$$\frac{1}{|V|} - N(0) \int_{-\omega_D}^0 \frac{d\epsilon}{\epsilon} \tanh \frac{\epsilon}{2T_c} = 0, \quad (2.9)$$

we can approximate

$$F(|\Delta|) - F(0) \approx \alpha(T_c - T) |\Delta|^2 + \beta |\Delta|^4, \quad (2.10)$$

where α and β are positive constants. This shows that the system is unstable to the BCS transition at temperatures be-

low T_c . In a similar way, we shall see below that T_s , the mean-field transition temperature into the $d+is$ state, is finite.

III. THE $d+is$ INSTABILITY

A. Formalism

We now need to develop the formalism that will enable us to extend the strategy from Sec. II to the $d+is$ case. We shall consider a single (two-dimensional) CuO_2 plane, and model it by the Hamiltonian

$$H = \int d^2r \sum_{\sigma=\uparrow,\downarrow} \psi_{\sigma}^{\dagger}(\mathbf{r}) \epsilon(-i\nabla) \psi_{\sigma}(\mathbf{r}) + \int d^2r d^2r' V(\mathbf{r}-\mathbf{r}') \psi_{\uparrow}^{\dagger}(\mathbf{r}) \psi_{\downarrow}^{\dagger}(\mathbf{r}') \psi_{\downarrow}(\mathbf{r}') \psi_{\uparrow}(\mathbf{r}), \quad (3.1)$$

where ϵ is the band energy and V is the short-range interaction responsible for pairing. What makes this difficult problem tractable is the separation of energy scales (the Fermi energy E_F is much bigger than the superconducting gap Δ), which gives rise to separation of length scales λ_F (Fermi wave length), and ξ (the coherence length). We may, therefore, expand in powers of the small parameter λ_F/ξ ; keeping the lowest nontrivial order is called the quasiclassical approximation. This procedure is usually done at the level of Green's function,^{6,20} which are thus transformed into Eilenberger functions that satisfy transportlike equations.

Since we want to understand the $d \rightarrow d+is$ transition in terms of quasiparticle eigenstates rather than Green's functions, we will perform this separation of scales at the operator level instead. We denote as 2Λ the width of the shell around the Fermi surface containing the states that take part in the pairing (see Fig. 2). We then factor out the fast Fermi-surface oscillations and define the slowly varying field operator $\psi_{\sigma,\theta}(\mathbf{r})$ (Ref. 21) by

$$\begin{aligned} \psi_{\sigma}(\mathbf{r}) &= \int \frac{d^2k}{(2\pi)^2} c_{\mathbf{k}\sigma} e^{i\mathbf{k}\cdot\mathbf{r}} \\ &\simeq \int_{\text{FS}} \frac{dk_F(\theta)}{2\pi} \left(\int_{-\Lambda}^{\Lambda} \frac{dk_{\perp}}{2\pi} c_{\mathbf{k}\sigma} e^{ik_{\perp}\mathbf{n}(\theta)\cdot\mathbf{r}} \right) e^{i\mathbf{k}_F(\theta)\cdot\mathbf{r}} \\ &\equiv \int_{\text{FS}} \frac{dk_F(\theta)}{2\pi} \psi_{\sigma,\theta}(\mathbf{r}) e^{i\mathbf{k}_F(\theta)\cdot\mathbf{r}}. \end{aligned} \quad (3.2)$$

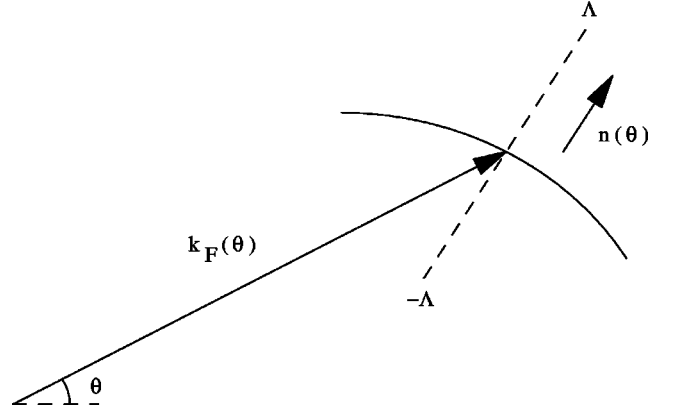


FIG. 2. Fermi-surface decomposition of the Fourier transform.

When we substitute this into Eq. (3.1), we obtain

$$\begin{aligned} H &= \int d^2r \left[\sum_{\sigma} \int_{\text{FS}} \frac{dk_F(\theta)}{2\pi} \psi_{\sigma,\theta}^{\dagger}(\mathbf{r}) \mathbf{v}_F(\theta) \cdot (-i\nabla) \psi_{\sigma,\theta}(\mathbf{r}) \right. \\ &\quad \left. + \int_{\text{FS}} \frac{dk_F(\theta)}{2\pi} \frac{dk_F(\theta')}{2\pi} V(\theta,\theta') \psi_{\uparrow,\theta}^{\dagger}(\mathbf{r}) \right. \\ &\quad \left. \times \psi_{\downarrow,-\theta}^{\dagger}(\mathbf{r}) \psi_{\downarrow,-\theta'}(\mathbf{r}) \psi_{\uparrow,\theta'}(\mathbf{r}) \right], \end{aligned} \quad (3.3)$$

where $\mathbf{v}_F(\theta)$ is the Fermi velocity at point $\mathbf{k}_F(\theta)$ and

$$V(\theta,\theta') \equiv \int d^2r e^{-i[\mathbf{k}_F(\theta)-\mathbf{k}_F(\theta')]\cdot\mathbf{r}} V(\mathbf{r}).$$

The derivation of Eq. (3.3) is given in Appendix A. Note the linearized kinetic energy in Eq. (3.3), which will be crucial in the following.

The Hamiltonian (3.3) gives rise to a partition function, which we can write as a path integral over the fermion fields $\psi_{\sigma,\theta}(\mathbf{r})$. We can again decompose the interaction by the HS transformation, i.e., we can multiply the partition function by the constant

$$\begin{aligned} &\int \mathcal{D}\bar{\phi}_{\theta}(\mathbf{r}) \mathcal{D}\phi_{\theta}(\mathbf{r}) \exp \left[\int_0^{\beta} d\tau \int d^2r \int_{\text{FS}} \frac{dk_F(\theta)}{2\pi} \frac{dk_F(\theta')}{2\pi} V(\theta,\theta') \right. \\ &\quad \left. \times [\bar{\phi}_{\theta}(\mathbf{r}) - \bar{\psi}_{\uparrow,\theta}(\mathbf{r}) \bar{\psi}_{\downarrow,-\theta}(\mathbf{r})] [\phi_{\theta'}(\mathbf{r}) - \psi_{\downarrow,-\theta'}(\mathbf{r}) \psi_{\uparrow,\theta'}(\mathbf{r})] \right]. \end{aligned} \quad (3.4)$$

In the mean-field approximation, the total free energy of the system equals the free energy given by the (single-particle) Hamiltonian

$$\begin{aligned}
H = & \int d^2r \left[\int_{\text{FS}} \frac{dk_F(\theta)}{2\pi} [\psi_{\uparrow\theta}^\dagger(\mathbf{r}) \psi_{\downarrow-\theta}(\mathbf{r}) \right. \\
& \times \begin{pmatrix} \mathbf{v}_F(\theta) \cdot (-i\nabla) & \Delta_\theta(\mathbf{r}) \\ \Delta_\theta^*(\mathbf{r}) & \mathbf{v}_F(\theta) \cdot (i\nabla) \end{pmatrix} \begin{pmatrix} \psi_{\uparrow\theta}(\mathbf{r}) \\ \psi_{\downarrow-\theta}^\dagger(\mathbf{r}) \end{pmatrix} \\
& \left. - \int_{\text{FS}} \frac{dk_F(\theta)}{2\pi} \frac{dk_F(\theta')}{2\pi} V(\theta, \theta') \phi_\theta^*(\mathbf{r}) \phi_{\theta'}(\mathbf{r}), \right. \\
& \left. (3.5) \right.
\end{aligned}$$

upon minimization with respect to $\phi_\theta(\mathbf{r})$, where we defined

$$\Delta_\theta(\mathbf{r}) = \int_{\text{FS}} \frac{dk_F(\theta')}{2\pi} V(\theta, \theta') \phi_{\theta'}(\mathbf{r}). \quad (3.6)$$

The minimization gives

$$\phi_\theta(\mathbf{r}) = \langle \psi_{\downarrow-\theta}(\mathbf{r}) \psi_{\uparrow\theta}(\mathbf{r}) \rangle, \quad (3.7)$$

where the angular brackets denote thermal average with respect to the Hamiltonian (3.5), see Appendix C. We shall write explicit formulas for the total energy and free energy in Sections IV and V [formulas (4.1) and (5.1)]. Here we just note that to calculate the single-particle contribution to the free energy, we will have to find the spectra of the Andreev Hamiltonians labeled by θ , i.e., we will need the energies $E_{\theta,n}$ that satisfy⁷

$$\begin{pmatrix} \mathbf{v}_F(\theta) \cdot (-i\nabla) & \Delta_\theta(\mathbf{r}) \\ \Delta_\theta^*(\mathbf{r}) & \mathbf{v}_F(\theta) \cdot (i\nabla) \end{pmatrix} \begin{pmatrix} f_{\theta,n}(\mathbf{r}) \\ g_{\theta,n}(\mathbf{r}) \end{pmatrix} = E_{\theta,n} \begin{pmatrix} f_{\theta,n}(\mathbf{r}) \\ g_{\theta,n}(\mathbf{r}) \end{pmatrix}. \quad (3.8)$$

We note that the linear kinetic energy in (3.3) makes this equation effectively one dimensional, i.e., an independent equation for each line in the direction $\mathbf{v}_F(\theta)$. In the presence of the specularly reflecting boundary, we must find the Andreev spectra along reflected lines such as the one in Fig. 1(a). Equivalently, we solve the equation on a straight line with the pairing potential Δ shown in Fig. 1(b). This is intuitively obvious; a derivation is given in Appendix B. For the pure d wave, we shall work in the gauge where Δ is real.

As we mentioned in the Introduction, the spectrum along each trajectory having opposite signs of Δ at the two asymptotic ends will contain a zero-bias state. Its wave function is, up to a normalization constant

$$\begin{pmatrix} f(\theta, \rho) \\ g(\theta, \rho) \end{pmatrix}_{\text{ZBS}} = \begin{pmatrix} 1 \\ \mp i \end{pmatrix} \exp\left(\mp \int_0^\rho d\rho' \Delta(\theta, \rho') / v_F(\theta)\right), \quad (3.9)$$

where the upper (lower) sign corresponds to $\Delta(\theta, \rho = -\infty) < 0$, $\Delta(\theta, \rho = +\infty) > 0$ [$\Delta(\theta, \rho = -\infty) > 0$, $\Delta(\theta, \rho = +\infty) < 0$], so that the wave function is normalizable. In our notation, we will freely interchange the dependence on \mathbf{r} (actually only on x , since the system is translationally invariant in

the y direction) with the dependence on the angle θ and the coordinate ρ along the trajectory. Their relationship is obvious from Fig. 1.

B. Argument

We now have all the tools needed to demonstrate the $d + is$ transition in a way that brings out its physical mechanism. We follow the same line of thought as in Sec. II: We go to the zero temperature, and look at the energy gains and losses when the s -wave component of Δ appears.

For any s -wave pairing to appear, it is necessary that the part of the functional integral (3.4) over the s component of ϕ converge, i.e., that V on top of the dominant d -wave attraction contain also an s -wave part (we use again $|V_s|$ rather than V_s)

$$V(\theta, \theta') = V_d(\theta, \theta') - |V_s|.$$

In this section, we will show that this condition is also sufficient: At zero temperature, the system will favor the $d + is$ state for an arbitrarily weak attraction V_s .

With both d - and s -wave pairing present,

$$\phi_\theta(\mathbf{r}) = \phi_{d\theta}(\mathbf{r}) + \phi_s(\mathbf{r}).$$

(The s components of both V and ϕ are angle independent.) We begin with the second term in Eq. (3.5), which then is

$$\begin{aligned}
& - \int_{\text{FS}} \frac{dk_F(\theta)}{2\pi} \frac{dk_F(\theta')}{2\pi} [V_d(\theta, \theta') - |V_s|] [\phi_{d\theta}^*(\mathbf{r}) + \phi_s^*(\mathbf{r})] \\
& \times [\phi_{d\theta'}(\mathbf{r}) + \phi_s(\mathbf{r})] \\
& = - \int_{\text{FS}} \frac{dk_F(\theta)}{2\pi} \frac{dk_F(\theta')}{2\pi} V_d(\theta, \theta') \phi_{d\theta}^*(\mathbf{r}) \phi_{d\theta'}(\mathbf{r}) \\
& + |V_s| \int_{\text{FS}} \frac{dk_F(\theta)}{2\pi} \frac{dk_F(\theta')}{2\pi} \phi_s^*(\mathbf{r}) \phi_s(\mathbf{r}), \quad (3.10)
\end{aligned}$$

where we used the orthogonality of the s and d components

$$\begin{aligned}
\int_{\text{FS}} \frac{dk_F(\theta)}{2\pi} V_d(\theta, \theta') &= \int_{\text{FS}} \frac{dk_F(\theta')}{2\pi} V_d(\theta, \theta') \\
&= \int_{\text{FS}} \frac{dk_F(\theta)}{2\pi} \phi_{d\theta}(\mathbf{r}) \\
&= 0.
\end{aligned}$$

We can also split up Eq. (3.6) into components and define

$$\Delta_{d\theta}(\mathbf{r}) = \int_{\text{FS}} \frac{dk_F(\theta')}{2\pi} V_d(\theta, \theta') \phi_{d\theta'}(\mathbf{r}),$$

$$\Delta_s(\mathbf{r}) = \int_{\text{FS}} \frac{dk_F(\theta)}{2\pi} (-|V_s|) \phi_s(\mathbf{r}). \quad (3.11)$$

The d component of Δ was established well above T_s , so the change of the second term in Eq. (3.5) due to the opening of a (small) s -wave gap will be

$$\frac{|\Delta_s(\mathbf{r})|^2}{|V_s|} \quad (3.12)$$

just as in the BCS case. Due to the translational invariance in the y direction, we will from now on write $\Delta_s(\mathbf{r}) \equiv \Delta_s(x)$. Along the quasiclassical trajectory, x depends on both ρ and θ (see Fig. 1), so we will then write $\Delta_s(\theta, \rho)$.

To examine the effect of the small s wave component on the quasiparticle energies, we need to look at the change of the spectra of the 1D Andreev problems

$$\begin{pmatrix} -iv_F(\theta)\partial_\rho & \Delta_d(\theta, \rho) \\ \Delta_d(\theta, \rho) & iv_F(\theta)\partial_\rho \end{pmatrix} \begin{pmatrix} f_n(\theta, \rho) \\ g_n(\theta, \rho) \end{pmatrix} = E_{\theta, n} \begin{pmatrix} f_n(\theta, \rho) \\ g_n(\theta, \rho) \end{pmatrix} \quad (3.13)$$

upon $\Delta_d(\theta, \rho) \rightarrow \Delta_d(\theta, \rho) + \Delta_s(\theta, \rho)$. As Δ_s is small, it can be treated as a perturbation; then the change of the quasiparticle energies to the lowest order is

$$\begin{aligned} E_{\theta, n}^{(1)}[\Delta_s] &= \int_{-\infty}^{+\infty} d\rho \begin{pmatrix} f_n^*(\theta, \rho) & g_n^*(\theta, \rho) \end{pmatrix} \\ &\times \begin{pmatrix} 0 & \Delta_s(\theta, \rho) \\ \Delta_s^*(\theta, \rho) & 0 \end{pmatrix} \begin{pmatrix} f_n(\theta, \rho) \\ g_n(\theta, \rho) \end{pmatrix} \\ &= \int_{-\infty}^{+\infty} d\rho [f_n^*(\theta, \rho)g_n(\theta, \rho)\Delta_s(\theta, \rho) \\ &+ g_n^*(\theta, \rho)f_n(\theta, \rho)\Delta_s^*(\theta, \rho)]. \end{aligned} \quad (3.14)$$

Let us first look at the change of energy of the zero-energy bound states. Then from Eq. (3.9)

$$g_{\text{ZBS}}(\theta, \rho) = \mp if_{\text{ZBS}}(\theta, \rho), \quad (3.15)$$

so

$$E_{\theta, \text{ZBS}}^{(1)}[\Delta_s] = \pm \int_{-\infty}^{+\infty} d\rho |f(\theta, \rho)|^2 2 \text{Im} \Delta_s(\theta, \rho), \quad (3.16)$$

where the upper (lower) sign corresponds to the $+y$ - ($-y$ -)moving trajectory. We notice several things by looking at Eq. (3.16).

It depends only on $\text{Im} \Delta_s$, since $\text{Re} \Delta_s$ just changes the position of the node in the total $\Delta(\theta, \rho)$, in which case the bound state remains at zero energy. Hence, we will assume $\text{Re} \Delta_s = 0$, and write $\Delta_s(\theta, \rho) = is(\theta, \rho)$.

$E_{\theta, \text{ZBS}}^{(1)}[\Delta_s]$ is nonzero due to the form of the bound-state wave function (3.15) and due to the fact that $s(\theta, \rho)$ does not change sign along the quasiclassical trajectory (by virtue of the s symmetry). Out of the two possibilities for the sign of s , we will choose $s(\theta, \rho) > 0$ in the following, which means all the $+y$ -moving states are shifted up in energy, whereas the $-y$ -moving states are shifted down.

Since we are at zero temperature, only the states that move down from zero energy will be occupied. We can then argue similarly as in the BCS case: opening of the additional s -wave gap costs the system energy $s^2/|V_s|$ [from Eq. (3.12)] but the quasiparticles save energy $\sim s$. The lowering of the

quasiparticle energy is only linear in s , i.e., not as dramatic as the nonanalytic decrease in the BCS case, but nevertheless it beats the quadratic increase for small enough s . Thus, for an arbitrarily small but nonzero interaction $|V_s|$, $s=0$ cannot be a minimum of the total energy, and the additional s -wave gap phase shifted by $\pi/2$ from the d -wave gap will appear. From the formula (3.16), we see that the superconductor will benefit from opening up the gap only close to the surface where $|f|^2$ is effectively nonzero, so the transition into the $d+is$ state is a surface effect. The decay into the bulk will be discussed more quantitatively in the next section.

We should also note that the remaining states on the quasiclassical trajectories do not change this situation, that is, they do not contribute linearly to the change of the total quasiparticle energy. Due to the time-reversal symmetry in the pure d -wave state, every state on a given quasiclassical trajectory corresponds to a state of the same energy on a reversed trajectory. Indeed, if we label the coordinate along the trajectory reversed to the one in Eq. (3.13) as $\tilde{\rho} = -\rho$, then the Hamiltonian on the reversed trajectory is

$$\begin{pmatrix} -iv_F(-\theta)\partial_{\tilde{\rho}} & \Delta_d(-\theta, \tilde{\rho}) \\ \Delta_d(-\theta, \tilde{\rho}) & iv_F(-\theta)\partial_{\tilde{\rho}} \end{pmatrix} = \begin{pmatrix} iv_F(\theta)\partial_\rho & \Delta_d(\theta, -\rho) \\ \Delta_d(\theta, -\rho) & -iv_F(\theta)\partial_\rho \end{pmatrix}$$

since $v_F(-\theta) = v_F(\theta)$, so

$$\begin{pmatrix} f_n(-\theta, \tilde{\rho}) \\ g_n(-\theta, \tilde{\rho}) \end{pmatrix} = \begin{pmatrix} g_n(\theta, -\rho) \\ f_n(\theta, -\rho) \end{pmatrix}$$

will also have energy $E_{\theta, n}$. Now Eq. (3.14) implies that to the first order, a small $\text{Im} \Delta_s$ will shift the energies of the two corresponding states by an equal amount with opposite signs. Hence, the only way they can linearly contribute to the total energy at $T=0$ is when one of them crosses zero and thus changes its occupancy, which happens only when their original energy (in absolute value) is smaller than the s -wave gap. But as $s \rightarrow 0$, there will be fewer and fewer such states in smaller and smaller neighborhoods of the d -wave nodes. It is only the ZBS's that change their occupancy for arbitrarily small s . We thus conclude that the onset of the transition into the $d+is$ state is driven by these states.

IV. s -WAVE GAP AT $T=0$

In the study of the instability of the pure d state in the last section, we used first-order perturbation theory since $s \rightarrow 0$ at the onset of $d+is$. Now we will argue that this theory holds up to the actual value of s , i.e., $s \ll |\Delta_d|$. As we will show in Sec. V, $s(T=0) \sim T_s$, the mean-field transition temperature into the $d+is$ state. Because $T_s \sim 7$ K, it is much smaller than T_d , the superconducting transition temperature of the order of 100 K, which sets the scale for Δ_d . Figure 3 shows the magnitude of the two gaps as a function of angle around a quarter of the Fermi surface. We see that the required inequality $s \ll |\Delta_d|$ holds for most of the Fermi surface

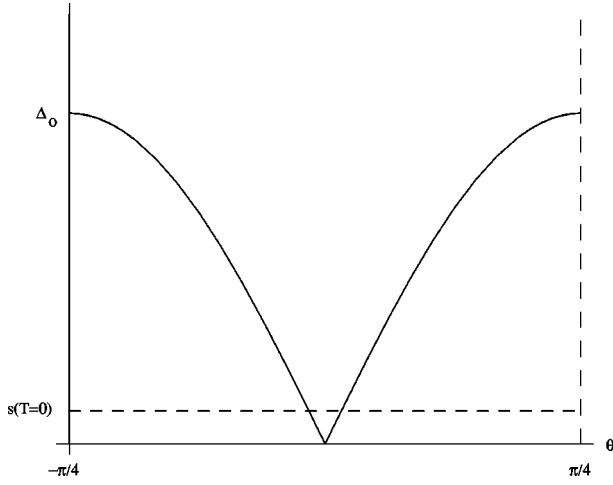


FIG. 3. The magnitude of the d - and s -wave order parameters around the Fermi surface.

except for small neighborhoods of the nodes. First-order perturbation theory certainly breaks down there, but upon averaging over the Fermi surface, the nodes will only introduce an error of the order T_s/T_d . Thus, we will use that theory to obtain $s(x)$ at $T=0$. As discussed at the end of Sec. III B, first-order perturbation theory implies that we have to look only at the zero-energy states. Also, since s is a small perturbation, we shall neglect its effect on Δ_d .

Now we can write down the energy due to s per unit length of the surface (the y direction) as a functional of $s(x)$:

$$E[s(x)] = \int_0^{+\infty} dx \frac{s^2(x)}{|V_s|} + \int_{\theta \in (-\pi/2, 0)} \frac{dk_F(\theta)}{2\pi} E_\theta[s(\theta, \rho)] \cos \theta, \quad (4.1)$$

where $E_\theta[s]$ is given by Eq. (3.16); for the rest of this section, we shall drop the superscript (1), since we shall be using only the first-order formula. We freely interchange $s(x)$ for $s(\theta, \rho)$; the relation between the two is discussed below Eq. (3.12). Note the correct dimensions: the x integration makes $s^2/|V_s|$ from energy per unit area into energy per unit length. In the second term, the integrand is energy and the dimension of the measure is k_F , i.e., inverse length. The extra factor of $\cos \theta$ in the second integral accounts for the difference of the density of trajectories along the y direction compared to their angle-independent intrinsic density (measured perpendicularly to their direction), as shown in Fig. 4. In the second term in Eq. (4.1), we sum up only the occupied $-y$ -moving states for which $E_\theta < 0$ according to Eq. (3.16).

We obtain $s(x)$ by minimizing Eq. (4.1). Let us first make an order-of-magnitude estimate

$$E[s] \sim \xi \frac{s^2}{|V_s|} - k_F s, \quad (4.2)$$

since s will extend into the bulk only as far as the coherence length $\xi = \hbar v_F / \Delta_0$ (Δ_0 is the amplitude of the d wave), and from Eq. (3.16), we see $E_\theta[s] \sim s$. The angular averaging

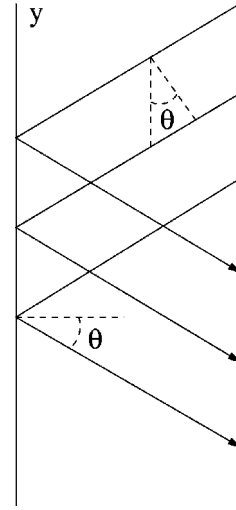


FIG. 4. The decrease of the density of the trajectories in the y direction by the factor $\cos \theta$.

will, up to numerical factors of order unity, multiply $E_\theta[s]$ by k_F . Minimization of Eq. (4.2) will give

$$s \sim \frac{k_F |V_s|}{\xi}. \quad (4.3)$$

By taking $s \sim 1$ meV from the experiment,¹² $k_F \sim 1 \text{ \AA}^{-1}$, and $\xi \sim 10 \text{ \AA}$, we get an estimate for the strength of the s -wave pairing

$$|V_s| \sim 10 \text{ meV \AA}^2.$$

We minimize Eq. (4.1) exactly by solving

$$\frac{\delta E[s]}{\delta s(x)} = 0,$$

i.e.,

$$2 \frac{s(x)}{|V_s|} - \int_{\theta \in (-\pi/2, 0)} \frac{dk_F(\theta)}{2\pi} \cos \theta \times \int_{-\infty}^{+\infty} d\rho 2|f(\theta, \rho)|^2 \frac{\delta s(\theta, \rho)}{\delta s(x)} = 0.$$

Now

$$\begin{aligned} \frac{\delta s(\theta, \rho)}{\delta s(x)} &= \delta(x - \rho \cos \theta) + \delta(x + \rho \cos \theta) \\ &= \frac{1}{\cos \theta} \left[\delta\left(\rho - \frac{x}{\cos \theta}\right) + \delta\left(\rho + \frac{x}{\cos \theta}\right) \right], \end{aligned} \quad (4.4)$$

since $\cos \theta > 0$, and ρ , unlike x , can be both positive and negative. The factors of $\cos \theta$ cancel, and we obtain

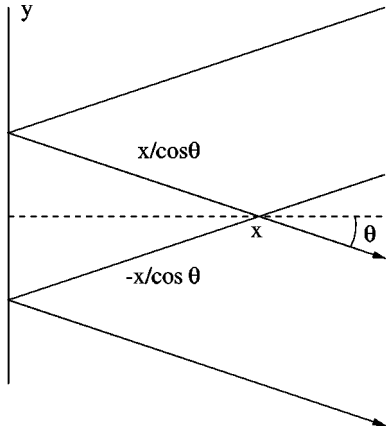


FIG. 5. Two contributions from the same θ to the pairing potential at the point x .

$$s(x) = |V_s| \int_{\theta \in (-\pi/2, 0)} \frac{dk_F(\theta)}{2\pi} \left[\left| f\left(\theta, \frac{x}{\cos\theta}\right) \right|^2 + \left| f\left(\theta, -\frac{x}{\cos\theta}\right) \right|^2 \right]. \quad (4.5)$$

Physically, we get two terms on the right-hand side because for each angle θ , there are two trajectories contributing to s at a given point as shown in Fig. 5.

We should remark here that we also obtain the formula (4.5) when we calculate the contribution from the occupied ($-y$ -moving) bound states to the pairing potential in the gap equation. This is done in Appendix C. The result is

$$\Delta_s(x)_{\text{ZBS}} = i|V_s| \int_{\theta \in (-\pi/2, 0)} \frac{dk_F(\theta)}{2\pi} \left[\left| f\left(\theta, \frac{x}{\cos\theta}\right) \right|^2 + \left| f\left(\theta, -\frac{x}{\cos\theta}\right) \right|^2 \right] \quad (4.6)$$

in agreement with Eq. (4.5). This formula, however, shows more clearly the internal consistency of the picture: For Δ_d in Fig. 1, the additional is potential pushes down the $-y$ -moving states if $s > 0$. As Eq. (4.6) shows, these states, in turn, give rise to $\Delta_s = i \times$ positive.

We should note here that Δ_s is absent on the right-hand side of Eq. (4.6), so the gap equation in this case (unlike in the BCS theory) is an explicit formula for the gap. The physical reason for this is that $s(x)$ is considered small, so we neglect the change of the bound-state wave functions due to its presence. The only effect of $s(x)$ we are taking into account is the change of the occupancy of the zero-energy states, which, by Eq. (3.16), depends only on the sign of s , not on its detailed shape. This is why $s(x)$ does not feed back into the right-hand side of Eq. (4.6).

To estimate the decay of Δ_s into the bulk, we shall assume Δ_d to be constant in space and with the angular dependence

$$\Delta_{d,\theta}(\mathbf{r}) = \Delta_0 \sin 2\theta, \quad (4.7)$$

which should hold for

$$x > \xi \equiv \frac{\hbar v_F}{\Delta_0}.$$

Also, we shall assume a spherical (circular) Fermi surface

$$dk_F(\theta) = k_F d\theta.$$

Then the wave function of the $-y$ -moving bound states, including the normalization, will be

$$\begin{pmatrix} f(\theta, \rho) \\ g(\theta, \rho) \end{pmatrix} = \sqrt{\frac{|\sin 2\theta|}{2\xi}} \begin{pmatrix} 1 \\ i \end{pmatrix} e^{-|\rho \sin 2\theta|/\xi}, \quad (4.8)$$

so

$$\begin{aligned} s(x) &= \frac{k_F |V_s|}{\xi} \int_{-\pi/2}^0 \frac{d\theta}{2\pi} 2 \times \frac{|\sin 2\theta|}{2} e^{-(2/\xi)(x/\cos\theta) \sin 2\theta} \\ &= \frac{k_F |V_s|}{\pi \xi} \int_0^{\pi/2} d\theta \sin \theta \cos \theta e^{-4 \sin \theta (x/\xi)}. \end{aligned} \quad (4.9)$$

We can do the integral by substitution $\sin \theta = t$, which gives

$$s(x) = \frac{k_F |V_s|}{\pi \xi} \left[-t \frac{\xi}{4x} - \left(\frac{\xi}{4x} \right)^2 e^{-4t(x/\xi)} \right]_{t=0}^1. \quad (4.10)$$

We can neglect the contribution from the upper limit because it is effectively nonzero only for $x < \xi/4$, where our assumption of constant Δ_d does not hold. The lower limit should have been at T_s/T_d , rather than at 0, to exclude the trajectories close to the nodes where the first-order perturbation theory breaks down. That cuts off the lower-bound contribution at $x \sim (T_d/4T_s)\xi \sim 100 \text{ \AA}$, beyond which we would need a more refined theory for the behavior of the quasiparticles around the nodes. For x much smaller than this distance, we can neglect the first term on the right hand side of Eq. (4.10), and replace the exponential by 1. We conclude, therefore, that

$$s(x) \simeq \frac{k_F |V_s| \xi}{16\pi x^2} \quad (4.11)$$

for

$$\xi < x \ll \frac{T_d}{T_s} \xi.$$

We see that $s = k_F |V_s|/\xi$ times a function that is of order unity for $x < \xi$, and decays fast for $x > \xi$, as expected.

V. TRANSITION TEMPERATURE

So far, we have shown the instability $d \rightarrow d + is$ only at $T = 0$. Just as in the BCS case, it remains to be demonstrated that the mean-field transition temperature T_s is finite. We therefore must study the free energy of the system, which we obtain from Eq. (4.1) when we replace $E_\theta[s]$ by $\mathcal{F}(E_\theta[s])$, the free energy of a single fermion level [see Eq. (2.6)], that is,

$$F[s] = \int_0^\infty dx \frac{s^2(x)}{|V_s|} + k_F \int_{-\pi/2}^{\pi/2} \frac{d\theta}{2\pi} \cos \theta (-T) \times \ln(1 + e^{-E_{\theta[s]}/T}). \quad (5.1)$$

Minimization of this functional will give an equation for $s(x)$ that again agrees with the contribution to the gap equation from the ZBS's. As we see from Eq. (5.1), the variational equation for s will now be very nonlinear; it will no longer be an explicit formula for s . The reason is that at finite temperatures, the occupancy of a given state depends on the value of its energy. Even in first-order perturbation theory, this value depends on the shape of $s(x)$, not just its sign, so $s(x)$ enters through the Fermi function into the right-hand side of the gap equation, making it nonlinear and therefore difficult to solve.

We still can make an order-of-magnitude estimate of F as follows:

$$\begin{aligned} & \ln(1 + e^{-E_{\theta[s]}/T}) + \ln(1 + e^{-E_{-\theta[s]}/T}) \\ &= \ln[(1 + e^{-E_{\theta[s]}/T})(1 + e^{E_{\theta[s]}/T})] \\ &= \ln\left(2 + 2 \cosh \frac{E_{\theta[s]}}{T}\right) \\ &\simeq \ln 4 + \frac{1}{4} \left(\frac{E_{\theta[s]}}{T}\right)^2 + O(E_{\theta[s]}^4) \\ &\sim \ln 4 + \frac{1}{4} \frac{s^2}{T^2} + O(s^4), \end{aligned}$$

so

$$F[s] - F[0] \sim s^2 \left(\frac{\xi}{|V_s|} - \frac{k_F}{T} \right) + O(s^4). \quad (5.2)$$

From Eq. (5.2) we see that the system is unstable to the transition to the $d+is$ state below the temperature $T_s \sim k_F |V_s| / \xi$, which is therefore of the same order of magnitude as $|\Delta_s|_{T=0}$. [see Eq. (4.3)].

Following Ref. 22, we can trade the coupling constant V_s for the transition temperature, T_{cs} of a BCS superconductor with this coupling $T_{cs} \sim e^{-1/|V_s|}$. Then

$$T_s \sim \frac{-1}{\ln T_{cs}}. \quad (5.3)$$

Hence, T_s increases sharply close to $T_{cs}=0$, which is consistent with the numerical results.^{5,13}

VI. CURRENT

To study the surface current in the $d+is$ state, we shall go back to $T=0$ for simplicity. We observe that the states on the $+y$ -moving quasiclassical trajectory from Fig. 1 will, upon the transition into the $d+is$ state with $s>0$, feel the pairing potential shown in Fig. 6. As ρ goes from $-\infty$ to $+\infty$, the twist of the phase φ of the order parameter is clockwise (from π to 0) for an $+y$ -moving trajectory and counterclockwise (from 0 to π) for a $-y$ -moving one. In both

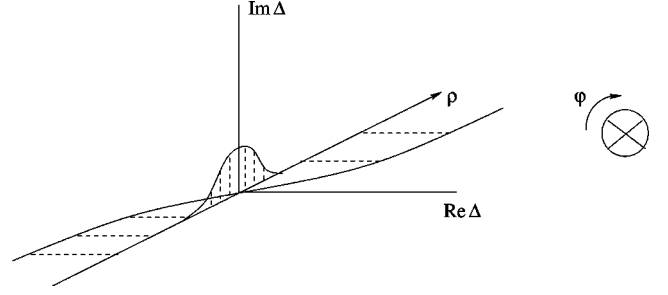


FIG. 6. The pairing potential along the trajectory in Fig. 1(a). The corresponding twist of the phase of the order parameter is clockwise.

cases, this implies current flowing in the $-y$ direction. This agrees with our previous calculations that showed that the $-y$ - ($+y$ -)moving bound states will be (un)occupied if $s > 0$.

The agreement is quantitative, as we can easily check. In the linearized Andreev formalism, the contribution to the current density from a given state is

$$j_n^{(1D)}(\theta, \rho) = ev_F (|f_n(\theta, \rho)|^2 + |g_n(\theta, \rho)|^2), \quad (6.1)$$

that is, the charge of the state times its (Fermi) velocity times the occupation of that state. In our case, all of the current is carried by the occupied bound states because the contributions from the remaining pairs of corresponding countermoving states cancel each other out (see the end of Sec. III B). To calculate the total current density in the y direction, we again have to include the contribution from both the incoming and the outgoing part of each $-y$ -moving trajectory (see Fig. 5), and we have to project onto the y direction

$$\begin{aligned} [j_{ZBS}(x)]_y &= k_F \int_{-\pi/2}^0 \frac{d\theta}{2\pi} \sin \theta \left[j_{ZBS}^{(1D)} \left(\theta, \frac{x}{\cos \theta} \right) \right. \\ &\quad \left. + j_{ZBS}^{(1D)} \left(\theta, -\frac{x}{\cos \theta} \right) \right]. \end{aligned} \quad (6.2)$$

On the other hand, in terms of the one-dimensional density $n^{(1D)} = k_F / \pi$ and the phase of the order parameter $\varphi(\theta, \rho)$ along the trajectory

$$j_{op}^{(1D)}(\theta, \rho) = e \frac{1}{2m} n^{(1D)} \partial_\rho \varphi(\theta, \rho) = \frac{ev_F}{2\pi} \partial_\rho \varphi(\theta, \rho), \quad (6.3)$$

since for a spherical Fermi surface $v_F = k_F / m$. The formula for the total surface-current density will be the same as Eq. (6.2), except that we now have to integrate over both $+y$ - and $-y$ -moving trajectories

$$\begin{aligned} [j_{OP}(x)]_y &= k_F \int_{-\pi/2}^{\pi/2} \frac{d\theta}{2\pi} \sin \theta \left[j_{OP}^{(1D)} \left(\theta, \frac{x}{\cos \theta} \right) \right. \\ &\quad \left. + j_{OP}^{(1D)} \left(\theta, -\frac{x}{\cos \theta} \right) \right]. \end{aligned} \quad (6.4)$$

We do not expect the current densities (6.2) and (6.4) to be the same at a given point because the formula (6.3) has corrections, which are higher-order derivatives of φ . Those corrections will not, however, contribute to the total surface current

$$I_y = \int_0^\infty dx j_y(x), \quad (6.5)$$

which should then come out the same in the two calculations. Indeed, the bound states give us

$$\begin{aligned} (I_{\text{ZBS}})_y &= k_F \int_{-\pi/2}^0 \frac{d\theta}{2\pi} \sin \theta \cos \theta \int_{-\infty}^{+\infty} d\rho j_{\text{ZBS}}^{(1\text{D})}(\theta, \rho), \\ &= -\frac{ev_F k_F}{4\pi}, \end{aligned} \quad (6.6)$$

since

$$\int_{-\infty}^{+\infty} d\rho j_{\text{ZBS}}^{(1\text{D})}(\theta, \rho) = ev_F$$

due to the normalization of the wave functions; the minus sign indicates that the current is flowing in the $-y$ direction. The formula for the total current in terms of the order-parameter phase is

$$(I_{\text{OP}})_y = k_F \int_{-\pi/2}^{\pi/2} \frac{d\theta}{2\pi} \sin \theta \cos \theta \int_{-\infty}^{+\infty} d\rho j_{\text{OP}}^{(1\text{D})}(\theta, \rho). \quad (6.7)$$

Now

$$\begin{aligned} \int_{-\infty}^{+\infty} d\rho j_{\text{OP}}^{(1\text{D})}(\theta, \rho) &= \frac{ev_F}{\pi} [\varphi(\theta, +\infty) - \varphi(\theta, -\infty)] \\ &= -\frac{ev_F}{2} \text{sgn}(\theta), \end{aligned} \quad (6.8)$$

so

$$(I_{\text{OP}})_y = -\frac{ev_F k_F}{4\pi} = (I_{\text{ZBS}})_y, \quad (6.9)$$

since $\text{sgn}(\theta)\sin\theta$ is an even function, so the factor 1/2 in Eq. (6.8) compensates for the doubling of the integration domain of θ in Eq. (6.4) compared to Eq. (6.2). To get an order-of-magnitude estimate, we put

$$e \sim 10^{-19} \text{ C},$$

$$v_F \sim 10^5 \text{ m/s},$$

$$k_F \sim 10^{10} \text{ m}^{-1},$$

and get $|I_y| \sim 10^{-5}$ A per CuO_2 plane. From the approximate form of the bound state wave functions introduced in the previous section, we can also estimate the spatial distribution of the current density

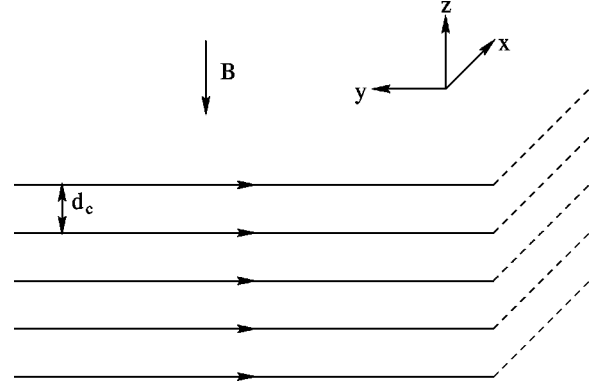


FIG. 7. Side view of the ab planes with the current flowing in the $-y$ direction. The induced magnetic field is along the c axis.

$$\begin{aligned} j_y(x) &= 4ev_F k_F \int_{-\pi/2}^0 \frac{d\theta}{2\pi} \sin \theta \left| f\left(\theta, \frac{x}{\cos \theta}\right) \right|^2 \\ &= -\frac{4ev_F k_F}{\xi} \int_0^{\pi/2} \frac{d\theta}{2\pi} \sin^2 \theta \cos \theta e^{-4(x/\xi)\sin \theta} \\ &= -\frac{2ev_F k_F}{\pi \xi} \int_0^1 dt t^2 e^{-(4x/\xi)t}. \end{aligned} \quad (6.10)$$

By the same argument as presented in the last section, we find that for $\xi < x \ll (T_d/T_s)\xi$,

$$j_y(x) \simeq -\frac{ev_F k_F}{16\pi \xi} \left(\frac{\xi}{x}\right)^3. \quad (6.11)$$

The extra power of x in the denominator in Eq. (6.11), compared to Eq. (4.11), comes from the directional sine in Eq. (6.2).

The surface current induces magnetic field, which will be screened by the diamagnetic current in the superconductor. The total current density therefore is

$$[j_{\text{tot}}(x)]_y = [j_{\text{ZBS}}(x)]_y + [j_{\text{dm}}(x)]_y. \quad (6.12)$$

According to Eq. (6.11), the current is localized within the distance $\sim \xi$ from the surface, which is much smaller than λ , the in-plane penetration depth, because the cuprates are strongly type-2 superconductors. Hence, the diamagnetic response does not resolve the internal structure of $[j_{\text{ZBS}}(x)]_y$, and we can estimate

$$[j_{\text{dm}}(x)]_y = [j_{\text{dm}}(0)]_y e^{-x/\lambda}. \quad (6.13)$$

The surface current will be screened completely, because the magnetic field it induces is smaller than B_{c1}^c , the lower critical field in the c direction. Indeed, even if the current flows in the same direction along all the CuO_2 planes (as shown in Fig. 7), the magnetic field at distances $x > d_c$ (the interplane spacing $\sim 10 \text{ \AA}$) from the surface will be

$$B = \frac{2\pi}{c} \frac{I}{d_c} \sim 10^2 \text{ G}, \quad (6.14)$$

which is smaller by an order of magnitude than B_{c1}^c for YBCO (see Ref. 23). The complete screening implies

$$(I_{\text{tot}})_y \equiv \int_0^\infty dx [j_{\text{tot}}(x)]_y = 0, \quad (6.15)$$

which together with Eq. (6.9) gives

$$[j_{dm}(0)]_y = \frac{e v_F k_F}{4 \pi \lambda}. \quad (6.16)$$

For $\xi < x \ll (T_d/T_s)\xi$, we can approximate the exponential in Eq. (6.13) by 1, so

$$[j_{\text{tot}}(x)]_y \simeq \frac{e v_F k_F}{16 \pi} \left[\frac{4}{\lambda} - \frac{1}{\xi} \left(\frac{\xi}{x} \right)^3 \right]. \quad (6.17)$$

This changes sign at distance

$$x_0 \sim \xi \kappa^{1/3}, \quad (6.18)$$

where $\kappa \equiv \lambda/\xi$ is the Ginzburg-Landau parameter. Due to the one-third power, $x_0 \sim \xi$ for reasonable values of κ (say, between 50 and 500). This is consistent with the numerical results.⁵

Note that the two calculations of the surface current agree [see Eq. (6.9)] because the ZBSs moving in the direction of the current are shifted down in energy and thus occupied, whereas those moving against the current are shifted up and unoccupied. We wish to stress that this is exactly *opposite* to the sign of the Doppler shift: the states moving along the current would be Doppler-shifted up, whereas those moving against the current would be Doppler-shifted down.

This point is further supported by the analogy between the ZBSs and low-lying excitations in a core of an *s*-wave vortex. We consider an idealized case: $\Delta = 0$ inside the vortex (at distances from the center smaller than R), and $|\Delta| = \text{const}$ outside with the phase winding counterclockwise once around. We look at a quasiclassical trajectory passing close to the center of the vortex. We denote the coordinate along the trajectory as ρ again and the phase at the intersection point with the vortex edge as φ_\pm , see Fig. 8. Then the energy of a low-lying excitation moving from $\rho = -\infty$ to $\rho = +\infty$ on that trajectory is²⁴

$$E = \frac{v_F}{4R} [(\varphi_+ - \varphi_-) - \pi]_{\text{mod } 2\pi}. \quad (6.19)$$

For a trajectory passing through the center, $\varphi_+ - \varphi_- = \pi$, so $E = 0$, and the low-lying excitation is a ZBS. If we now shift the trajectory slightly to the left as shown in Fig. 8, then $\varphi_+ - \varphi_- > \pi$ and $E > 0$. In a real vortex, Δ would be non-zero even inside, and the phase of Δ would wind clockwise as we go from $\rho = -\infty$ to $\rho = +\infty$, so we are going against the current. Moreover, $\varphi(\rho = +\infty) - \varphi(\rho = -\infty) = \pi \text{ mod } 2\pi$, so Δ behaves the same way as in Fig. 6. Hence, the $d \rightarrow d+is$ transition is analogous to shifting the quasiclassical trajectory away from the vortex center. In both cases, the ZBS will have a positive energy if it is moving against the current and negative energy if it is moving in the direction of the current.

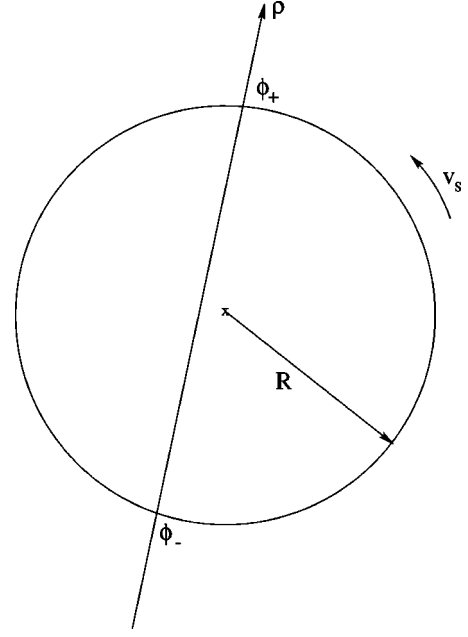


FIG. 8. A quasiclassical trajectory going through the core of an *s*-wave vortex.

VII. DISCUSSION

In order to understand the basic physical mechanism of the $d \rightarrow d+is$ transition, we considered the change of the free energy of a CuO_2 half-plane when an *s*-wave component of Δ appears close to the 110 surface. By the Hubbard-Stratonovich transformation and the mean-field approximation, we decomposed the total free energy into the contribution from the single-particle states, which is decreased by $\text{Im } \Delta_s$, and the HS term, which increases quadratically with Δ_s . Using first-order perturbation theory, we saw that the system favors the $d+is$ state at $T=0$, and that the transition is driven by the zero-bias states. Based on this argument and on the separation of energy scales associated with the *d*- and *s*-wave components of Δ , we then calculated Δ_s at zero temperature and estimated the transition temperature. Finally, we discussed the surface current in the $d+is$ state. We saw that it is carried by the occupied ZBSs; these states are *not* Doppler-shifted by the current. This current could be demonstrated experimentally by Andreev reflection.²⁵

In the Introduction, we mentioned various improvements that would make the model more realistic, such as magnetic domains, interlayer coupling, and going beyond quasiclassical approximation or mean-field theory. Before developing the model further, it would be worthwhile to reexamine its assumptions, especially the *d*-wave symmetry of the dominant order parameter in light of various recent experimental results in support of *s*-wave symmetry.²⁶

ACKNOWLEDGMENTS

I want to give special thanks to M. Stone for suggesting the problem and discussing it with me. I wish to thank A.J. Leggett for helping me figure out the diamagnetic response in Sec. VI. I have also benefited from discussions with I.

Adagideli, H. Aubin, L.H. Greene, R.A. Klemm, D.E. Pugel, R. Ramazashvili, S. Sachdev, M. Turlakov, and H. Westfahl. I am grateful to C. Elliott for proofreading the manuscript. The project was supported by Grant No. NSF-DMR-98-17941.

APPENDIX A: DERIVATION OF THE QUASICLASSICAL HAMILTONIAN

We derive Eq. (3.3) from Eq. (3.1) by expressing the original field $\psi_\sigma(\mathbf{r})$ in terms of the slowly varying field $\psi_{\sigma\theta}(\mathbf{r})$, see (3.2). We first substitute into the kinetic-energy operator

$$\begin{aligned} \epsilon(-i\nabla)\psi_\sigma(\mathbf{r}) &= \int_{\text{FS}} \frac{dk_F(\theta)}{2\pi} e^{i\mathbf{k}_F(\theta)\cdot\mathbf{r}} \epsilon(\mathbf{k}_F(\theta) - i\nabla)\psi_{\sigma,\theta}(\mathbf{r}) \\ &= \int_{\text{FS}} \frac{dk_F(\theta)}{2\pi} e^{i\mathbf{k}_F(\theta)\cdot\mathbf{r}} \{ \epsilon(\mathbf{k}_F(\theta)) \\ &\quad + \nabla_{\mathbf{k}}\epsilon(\mathbf{k})|_{\mathbf{k}_F(\theta)} \cdot (-i\nabla) + \dots \} \psi_{\sigma,\theta}(\mathbf{r}) \\ &\simeq \int_{\text{FS}} \frac{dk_F(\theta)}{2\pi} e^{i\mathbf{k}_F(\theta)\cdot\mathbf{r}} \mathbf{v}_F(\theta) \cdot (-i\nabla)\psi_{\sigma,\theta}(\mathbf{r}), \end{aligned} \quad (\text{A1})$$

since

$$\epsilon(\mathbf{k}_F) = 0, \quad \text{and} \quad \nabla_{\mathbf{k}}\epsilon(\mathbf{k})|_{\mathbf{k}_F} = \mathbf{v}_F.$$

The kinetic energy therefore is

$$\begin{aligned} &\int d^2r \sum_{\sigma=\uparrow,\downarrow} \psi_\sigma^\dagger(\mathbf{r}) \epsilon(-i\nabla)\psi_\sigma(\mathbf{r}) \\ &= \int d^2r \sum_{\sigma} \int_{\text{FS}} \frac{dk_F(\theta)}{2\pi} \int_{\text{FS}} \frac{dk_F(\theta')}{2\pi} e^{i[\mathbf{k}_F(\theta) - \mathbf{k}_F(\theta')]\cdot\mathbf{r}} \\ &\quad \times \psi_{\sigma,\theta'}^\dagger(\mathbf{r}) \mathbf{v}_F(\theta) \cdot (-i\nabla)\psi_{\sigma,\theta}(\mathbf{r}). \end{aligned} \quad (\text{A2})$$

Now $e^{i[\mathbf{k}_F(\theta) - \mathbf{k}_F(\theta')]\cdot\mathbf{r}}$ oscillates with a wavelength much shorter than the length scale on which $\psi_{\sigma,\theta}(\mathbf{r})$ changes. Thus, the integral will be zero unless $\mathbf{k}_F(\theta) - \mathbf{k}_F(\theta') = 0$, so we can effectively drop one integration over the Fermi surface, and obtain the kinetic energy of the form

$$\int d^2r \sum_{\sigma} \int_{\text{FS}} \frac{dk_F(\theta)}{2\pi} \psi_{\sigma,\theta}^\dagger(\mathbf{r}) \mathbf{v}_F(\theta) \cdot (-i\nabla)\psi_{\sigma,\theta}(\mathbf{r}). \quad (\text{A3})$$

The potential energy is now given by

$$\begin{aligned} &\int d^2r d^2r' \frac{dk_F(\theta_1)}{2\pi} \frac{dk_F(\theta_2)}{2\pi} \frac{dk_F(\theta_3)}{2\pi} \frac{dk_F(\theta_4)}{2\pi} V(\mathbf{r} - \mathbf{r}') \exp\{i[-\mathbf{k}_F(\theta_1)\cdot\mathbf{r} - \mathbf{k}_F(\theta_2)\cdot\mathbf{r}' + \mathbf{k}_F(\theta_3)\cdot\mathbf{r}' + \mathbf{k}_F(\theta_4)\cdot\mathbf{r}]\} \\ &\quad \times \psi_{\uparrow\theta_1}^\dagger(\mathbf{r}) \psi_{\downarrow\theta_2}^\dagger(\mathbf{r}') \psi_{\uparrow\theta_3}(\mathbf{r}') \psi_{\uparrow\theta_4}(\mathbf{r}) \\ &\approx \int d^2r d^2r' \frac{dk_F(\theta_1)}{2\pi} \frac{dk_F(\theta_2)}{2\pi} \frac{dk_F(\theta_3)}{2\pi} \frac{dk_F(\theta_4)}{2\pi} V(\mathbf{r} - \mathbf{r}') e^{i[\mathbf{k}_F(\theta_2) - \mathbf{k}_F(\theta_3)]\cdot(\mathbf{r} - \mathbf{r}')} \psi_{\uparrow\theta_1}^\dagger(\mathbf{r}) \psi_{\downarrow\theta_2}^\dagger(\mathbf{r}') \psi_{\uparrow\theta_3}(\mathbf{r}') \psi_{\uparrow\theta_4}(\mathbf{r}) \\ &\quad \times \exp\{i[-\mathbf{k}_F(\theta_1) - \mathbf{k}_F(\theta_2) + \mathbf{k}_F(\theta_3) + \mathbf{k}_F(\theta_4)]\cdot\mathbf{r}\} \\ &= \int d^2r d^2r' \frac{dk_F(\theta_1)}{2\pi} \frac{dk_F(\theta_2)}{2\pi} \frac{dk_F(\theta_3)}{2\pi} \frac{dk_F(\theta_4)}{2\pi} V(\theta_2, \theta_3) \psi_{\uparrow\theta_1}^\dagger(\mathbf{r}) \psi_{\downarrow\theta_2}^\dagger(\mathbf{r}') \psi_{\uparrow\theta_3}(\mathbf{r}') \psi_{\uparrow\theta_4}(\mathbf{r}) \\ &\quad \times \exp\{i[-\mathbf{k}_F(\theta_1) - \mathbf{k}_F(\theta_2) + \mathbf{k}_F(\theta_3) + \mathbf{k}_F(\theta_4)]\cdot\mathbf{r}\}, \end{aligned} \quad (\text{A4})$$

where we used the assumption that V changes on a much shorter length scale than $\psi_{\sigma,\theta}(\mathbf{r})$, performed the r' integration, and introduced the Fourier transform

$$V(\theta, \theta') \equiv \int d^2r e^{-i[\mathbf{k}_F(\theta) - \mathbf{k}_F(\theta')]\cdot\mathbf{r}} V(\mathbf{r}).$$

Since $V(\mathbf{r}) = V(-\mathbf{r})$, we see that $V(\theta, \theta') = V(\theta', \theta)$. Again, the integral vanishes unless the sum of the four momenta is zero. Out of the various ways that this may happen, we pick only the one that contributes to the singlet pairing, namely,

$$\mathbf{k}_F(\theta_1) + \mathbf{k}_F(\theta_2) = \mathbf{k}_F(\theta_3) + \mathbf{k}_F(\theta_4) = 0, \quad \text{i.e.,}$$

$$\theta_1 + \theta_2 = \theta_3 + \theta_4 = 0 \pmod{2\pi}. \quad (\text{A5})$$

Since we now have two constraints, we can drop two Fermi-surface integrations, and obtain the potential energy of the form

$$\begin{aligned} &\int d^2r \frac{dk_F(\theta)}{2\pi} \frac{dk_F(\theta')}{2\pi} V(\theta, \theta') \psi_{\uparrow\theta}^\dagger \\ &\quad \times (\mathbf{r}) \psi_{\downarrow-\theta}^\dagger(\mathbf{r}) \psi_{\downarrow-\theta'}(\mathbf{r}) \psi_{\uparrow\theta'}(\mathbf{r}). \end{aligned}$$

The total Hamiltonian in the quasiclassical approximation then is

$$H = \int d^2r \left[\sum_{\sigma} \int_{\text{FS}} \frac{dk_F(\theta)}{2\pi} \psi_{\sigma,\theta}^{\dagger}(\mathbf{r}) \mathbf{v}_F(\theta) \cdot (-i\nabla) \psi_{\sigma,\theta}(\mathbf{r}) + \int_{\text{FS}} \frac{dk_F(\theta)}{2\pi} \frac{dk_F(\theta')}{2\pi} V(\theta, \theta') \psi_{\uparrow\theta}^{\dagger}(\mathbf{r}) \times \psi_{\downarrow-\theta}^{\dagger}(\mathbf{r}) \psi_{\downarrow-\theta'}(\mathbf{r}) \psi_{\uparrow\theta'}(\mathbf{r}) \right]. \quad (\text{A6})$$

The derivation of Eq. (A6) from Eq. (3.1) is far from rigorous. We could give a somewhat better, although much longer, argument. We believe the approximations used here are equivalent to the approximation in the Eilenberger formalism, because the Eilenberger equations can now be rigorously (apart from the mean-field approximation) derived from Eq. (A6).

APPENDIX B: BOUNDARY CONDITIONS AT THE SURFACE

We show the effect of the boundary on the Andreev spectrum. In general, the boundary will cause mixing of different θ 's. For each θ , though, we have a different Andreev equation, so adding the solutions of Eq. (3.8) for different θ 's does not make sense. However, the Andreev wave functions describe only the slow variation of our excitations (changes on the length scale ξ). The full wave functions containing the rapid oscillations as well are

$$\begin{pmatrix} f_{\theta,n}(\mathbf{r}) \\ g_{\theta,n}(\mathbf{r}) \end{pmatrix} e^{i\mathbf{k}_F(\theta) \cdot \mathbf{r}}, \quad (\text{B1})$$

and these describe the single-particle excitations of the *same* Hamiltonian (3.1) (in the mean-field approximation), so those can be added. If we assume a specularly reflecting boundary, then the wave function will contain only two terms

$$\begin{pmatrix} f_{\theta_{\text{in}},n}(\mathbf{r}) \\ g_{\theta_{\text{in}},n}(\mathbf{r}) \end{pmatrix} e^{i\mathbf{k}_F(\theta_{\text{in}}) \cdot \mathbf{r}} + \begin{pmatrix} f_{\theta_{\text{out}},n}(\mathbf{r}) \\ g_{\theta_{\text{out}},n}(\mathbf{r}) \end{pmatrix} e^{i\mathbf{k}_F(\theta_{\text{out}}) \cdot \mathbf{r}},$$

such that

$$\theta_{\text{in}} + \theta_{\text{out}} = \pi \pmod{2\pi}, \quad (\text{B2})$$

since the angles are measured from the positive- x semiaxis, see Fig. 1(a). The Dirichlet boundary condition gives

$$\begin{pmatrix} f_{\theta_{\text{out}},n}(\mathbf{r}) \\ g_{\theta_{\text{out}},n}(\mathbf{r}) \end{pmatrix} = \begin{pmatrix} f_{\theta_{\text{in}},n}(\mathbf{r}) \\ g_{\theta_{\text{in}},n}(\mathbf{r}) \end{pmatrix} (-e^{i[\mathbf{k}_F(\theta_{\text{in}}) - \mathbf{k}_F(\theta_{\text{out}})] \cdot \mathbf{r}})_{\mathbf{r} \in \text{surface}},$$

whereas the Neumann boundary condition gives

$$\begin{pmatrix} f_{\theta_{\text{out}},n}(\mathbf{r}) \\ g_{\theta_{\text{out}},n}(\mathbf{r}) \end{pmatrix} = \begin{pmatrix} f_{\theta_{\text{in}},n}(\mathbf{r}) \\ g_{\theta_{\text{in}},n}(\mathbf{r}) \end{pmatrix} (e^{i[\mathbf{k}_F(\theta_{\text{in}}) - \mathbf{k}_F(\theta_{\text{out}})] \cdot \mathbf{r}})_{\mathbf{r} \in \text{surface}}$$

since

$$\mathbf{n} \cdot [\mathbf{k}_F(\theta_{\text{in}}) - \mathbf{k}_F(\theta_{\text{out}})] = 0$$

for \mathbf{n} perpendicular to the surface, and we used

$$k_F \begin{pmatrix} f \\ g \end{pmatrix} \gg \mathbf{n} \cdot \nabla_r \begin{pmatrix} f \\ g \end{pmatrix}$$

to neglect the gradient of the Andreev wave function. Since Eq. (3.8) is linear, we can drop multiplicative constants and simply assume

$$\begin{pmatrix} f_{\theta_{\text{out}},n}(\mathbf{r}) \\ g_{\theta_{\text{out}},n}(\mathbf{r}) \end{pmatrix} = \begin{pmatrix} f_{\theta_{\text{in}},n}(\mathbf{r}) \\ g_{\theta_{\text{in}},n}(\mathbf{r}) \end{pmatrix} \quad (\text{B3})$$

at the surface for either choice of the boundary condition. As θ_{in} is uniquely determined by θ_{out} through the relation (B2), we shall label the potential Δ along the trajectory as well as the solutions of the corresponding Andreev equation by θ_{out} . We shall drop the subscript out everywhere except in Appendix C, where we will need to distinguish θ_{out} , the label for a trajectory as in Fig. 1, from θ , the label for a position on the Fermi surface as in Fig. 2.

APPENDIX C: GAP EQUATION

We obtain the gap equation by substituting for $\phi_{\theta}(\mathbf{r})$ in Eq. (3.6) its mean-field value, that is, the pairing amplitude $\phi_{\theta}(\mathbf{r}) \equiv \langle \psi_{\downarrow-\theta}(\mathbf{r}) \psi_{\uparrow\theta}(\mathbf{r}) \rangle$. To calculate this amplitude, we expand the field operators into energy eigenstates

$$\begin{pmatrix} \psi_{\uparrow\theta}(\mathbf{r}) \\ \psi_{\downarrow-\theta}^{\dagger}(\mathbf{r}) \end{pmatrix} = \sum_n \gamma_{\theta,n} \begin{pmatrix} f_n(\theta, \rho) \\ g_n(\theta, \rho) \end{pmatrix}. \quad (\text{C1})$$

Equation (C1) gives at $T=0$

$$\begin{aligned} \langle \psi_{\downarrow-\theta}(\mathbf{r}) \psi_{\uparrow\theta}(\mathbf{r}) \rangle &= \sum_{n,n'} f_n(\theta, \rho) g_{n'}^*(\theta, \rho) \langle \gamma_{\theta,n'}^{\dagger} \gamma_{\theta,n} \rangle \\ &= \sum_n \Theta(-E_{\theta,n}) f_n(\theta, \rho) g_n^*(\theta, \rho). \end{aligned} \quad (\text{C2})$$

Note that in Eq. (C1), we explicitly sum over both positive and negative energies, unlike the Bogoliubov–de Gennes (BdG) formalism where we can sum over positive energies only, using the fact that

$$\begin{pmatrix} u_n(\mathbf{r}) \\ v_n(\mathbf{r}) \end{pmatrix} \quad \text{and} \quad \begin{pmatrix} -v_n^*(\mathbf{r}) \\ u_n^*(\mathbf{r}) \end{pmatrix} \quad (\text{C3})$$

are both solutions of the BdG equations with energies equal in absolute value and opposite in sign. However, this sym-

metry is lost here because the Andreev wave functions corresponding to the BdG wave functions (C3) live on different quasiclassical trajectories.

Close to the surface, we have to remember again that each line contributes to the pairing amplitude at a given point for two directions θ ; see Fig. 5. We will, therefore, have to distinguish between the label of the trajectory θ_{out} and the label for the pairing amplitude θ . Specifically,

$$\begin{aligned} \theta_{\text{out}} &= \theta \quad \text{for } \theta \in \left(-\frac{\pi}{2}, 0\right) \text{ and} \\ \theta_{\text{out}} &= -\pi - \theta \quad \text{for } \theta \in \left(-\pi, -\frac{\pi}{2}\right), \end{aligned} \quad (\text{C4})$$

so the contribution to the pairing amplitude from the $-y$ -moving bound states will be

$$\begin{aligned} \langle \psi_{\downarrow-\theta}(\mathbf{r}) \psi_{\uparrow\theta}(\mathbf{r}) \rangle_{\text{ZBS}} &= f\left(\theta_{\text{out}}, \frac{x}{\cos \theta_{\text{out}}}\right) g^*\left(\theta_{\text{out}}, \frac{x}{\cos \theta_{\text{out}}}\right) \\ &= f\left(\theta, \frac{x}{\cos \theta}\right) g^*\left(\theta, \frac{x}{\cos \theta}\right) \end{aligned}$$

for

$$\theta \in \left(-\frac{\pi}{2}, 0\right) \quad (\text{C5})$$

and

$$\begin{aligned} \langle \psi_{\downarrow-\theta}(\mathbf{r}) \psi_{\uparrow\theta}(\mathbf{r}) \rangle_{\text{ZBS}} &= f\left(\theta_{\text{out}}, -\frac{x}{\cos \theta_{\text{out}}}\right) g^*\left(\theta_{\text{out}}, -\frac{x}{\cos \theta_{\text{out}}}\right) \\ &= f\left(-\pi - \theta, \frac{x}{\cos \theta}\right) g^*\left(-\pi - \theta, \frac{x}{\cos \theta}\right) \end{aligned}$$

for

$$\theta \in \left(-\pi, -\frac{\pi}{2}\right). \quad (\text{C6})$$

Substituting Eqs. (C5) and (C6) into Eq. (3.6) gives

$$\begin{aligned} \Delta_{\theta}(x)_{\text{ZBS}} &= \int_{\theta' \in (-\pi, 0)} \frac{dk_F(\theta')}{2\pi} V(\theta, \theta') \\ &\quad \times \langle \psi_{\downarrow-\theta'}(\mathbf{r}) \psi_{\uparrow\theta'}(\mathbf{r}) \rangle_{\text{ZBS}} \\ &= \int_{\theta'_{\text{out}} \in (-\pi/2, 0)} \frac{dk_F(\theta'_{\text{out}})}{2\pi} \left[V(\theta, \theta'_{\text{out}})(-i) \right. \\ &\quad \times \left| f\left(\theta'_{\text{out}}, \frac{x}{\cos \theta'_{\text{out}}}\right) \right|^2 + V(\theta, -\pi - \theta'_{\text{out}})(-i) \\ &\quad \left. \times \left| f\left(\theta'_{\text{out}}, -\frac{x}{\cos \theta'_{\text{out}}}\right) \right|^2 \right], \end{aligned} \quad (\text{C7})$$

where

$$V(\theta, \theta'_{\text{out}}) = -|V_s| + V_d(\theta, \theta'_{\text{out}}),$$

and we used Eq. (3.15). The contribution to the s -wave component of the pairing potential from the occupied bound states therefore is

$$\begin{aligned} \Delta_s(x)_{\text{ZBS}} &= i|V_s| \int_{\theta'_{\text{out}} \in (-\pi/2, 0)} \frac{dk_F(\theta'_{\text{out}})}{2\pi} \left[\left| f\left(\theta'_{\text{out}}, \frac{x}{\cos \theta'_{\text{out}}}\right) \right|^2 \right. \\ &\quad \left. + \left| f\left(\theta'_{\text{out}}, -\frac{x}{\cos \theta'_{\text{out}}}\right) \right|^2 \right]. \end{aligned} \quad (\text{C8})$$

For the calculation of the d -wave component of Δ_{ZBS} , we will assume that the unperturbed Δ_d is antisymmetric around its vertical node

$$\Delta_{d,\theta}(\mathbf{r}) = -\Delta_{d,-\pi-\theta}(\mathbf{r}). \quad (\text{C9})$$

Presumably, Δ_d arises from an antisymmetric interaction

$$V_d(\theta, \theta') = -V_d(\theta, -\pi - \theta'). \quad (\text{C10})$$

Along the quasiclassical trajectory, Eq. (C9) means

$$\Delta_d(\theta, \rho) = -\Delta_d(\theta, -\rho), \quad (\text{C11})$$

which, by Eq. (3.9), implies

$$|f(\theta, \rho)|^2 = |f(\theta, -\rho)|^2. \quad (\text{C12})$$

Thus, under these assumptions,

$$\begin{aligned} \Delta_{d,\theta}(x)_{\text{ZBS}} &= (-i) \int_{\theta'_{\text{out}} \in (-\pi/2, 0)} \frac{dk_F(\theta'_{\text{out}})}{2\pi} [V_d(\theta, \theta'_{\text{out}}) \\ &\quad + V_d(\theta, -\pi - \theta'_{\text{out}})] \left| f\left(\theta'_{\text{out}}, \frac{x}{\cos \theta'_{\text{out}}}\right) \right|^2 = 0. \end{aligned} \quad (\text{C13})$$

- ¹D.J. Van Harlingen, *Rev. Mod. Phys.* **67**, 515 (1995).
- ²M.F. Atiyah, V.K. Patodi, and I.M. Singer, *Proc. Cambridge Philos. Soc.* **77**, 43 (1975).
- ³C.R. Hu, *Phys. Rev. Lett.* **72**, 1526 (1994).
- ⁴M. Matsumoto and H. Shiba, *J. Phys. Soc. Jpn.* **64**, 3384 (1995); **64**, 4867 (1995).
- ⁵M. Fogelström, D. Rainer, and J.A. Sauls, *Phys. Rev. Lett.* **79**, 281 (1997).
- ⁶G. Eilenberger, *Z. Phys.* **214**, 195 (1968).
- ⁷A.F. Andreev, *Zh. Éksp. Teor. Fiz.* **46**, 1823 (1964) [*Sov. Phys. JETP* **19**, 1228 (1964)].
- ⁸J. Geerk, X.X. Xi, and G. Linker, *Z. Phys. B: Condens. Matter* **73**, 329 (1988).
- ⁹J. Lesueur, L.H. Greene, W.L. Feldman, and A. Inam, *Physica C* **191**, 325 (1992).
- ¹⁰S. Kashiwaya, Y. Tanaka, M. Koyanagi, H. Takashima, and K. Kajimura, *Phys. Rev. B* **51**, 1350 (1995).
- ¹¹M. Covington, R. Scheuerer, K. Bloom, and L.H. Greene, *Appl. Phys. Lett.* **68**, 1717 (1996).
- ¹²M. Covington, M. Aprili, E. Paraoanu, L.H. Greene, F. Xu, J. Zhu, and C.A. Mirkin, *Phys. Rev. Lett.* **79**, 277 (1997).
- ¹³D. Rainer, H. Burkhardt, M. Fogelström, and J.A. Sauls, *J. Phys. Chem. Solids* **59**, 2040 (1998).
- ¹⁴W.K. Neils, B.L.T. Plourde, and D.J. Van Harlingen, *Physica C* **341-348**, 1705 (2000); W.K. Neils and D.J. Van Harlingen, *Physica B* **284**, 587 (2000).
- ¹⁵J. Annett, N. Goldenfeld, and A.J. Leggett, in *Physical Properties of High Temperature Superconductors*, edited by D.M. Ginsberg (World Scientific, Singapore, 1996), pp. 375–461.
- ¹⁶R.A. Klemm, C.T. Rieck, and K. Scharnberg, *Phys. Rev. B* **61**, 5913 (2000).
- ¹⁷R. Kleiner, A.S. Katz, A.G. Sun, R. Summer, D.A. Gajewski, S.H. Han, S.I. Woods, E. Dantsker, B. Chen, K. Char, M.B. Maple, R.C. Dynes, and John Clarke, *Phys. Rev. Lett.* **76**, 2161 (1996).
- ¹⁸A.G. Sun, A. Truscott, A.S. Katz, R.C. Dynes, B.W. Veal, and C. Gu, *Phys. Rev. B* **54**, 6734 (1996).
- ¹⁹D.E. Pugel, M.B. Salamon, M.B. Weissman, and L.H. Greene (unpublished).
- ²⁰J.W. Serene and D. Rainer, *Phys. Rep.* **101**, 221 (1983).
- ²¹M. Stone and F. Gaitan, *Ann. Phys. (N.Y.)* **178**, 89 (1987).
- ²²L.J. Buchholtz, M. Palumbo, D. Rainer, and J.A. Sauls, *J. Low Temp. Phys.* **101**, 1079 (1995); **101**, 1099 (1995).
- ²³C.P. Poole, Jr., H.A. Farach, and R.J. Creswick, *Superconductivity* (Academic Press, New York, 1995), p. 290.
- ²⁴M. Stone, *Phys. Rev. B* **54**, 13 222 (1996).
- ²⁵B. Götzelmann, S. Hoffmann, and R. Kümmel, *Phys. Rev. B* **52**, R3848 (1995).
- ²⁶P. Chaudhari and S.-Y. Lin, *Phys. Rev. Lett.* **72**, 1084 (1994); A. Bhattacharya, I. Zutic, O.T. Valls, A.M. Goldman, U. Welp, and B. Veal, *ibid.* **82**, 3132 (1999); Q. Li, Y.N. Tsay, M. Suenaga, R.A. Klemm, G.D. Gu, and N. Koshizuka, *ibid.* **83**, 4160 (1999); S.H. Pan, E.W. Hudson, A.K. Gupta, K-W. Ng, H. Eisaki, S. Uchida, and J.C. Davis, cond-mat/0005484 (unpublished).